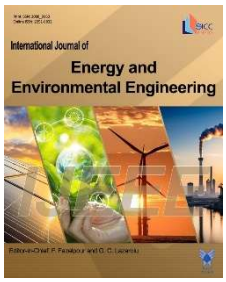

Volume 16, Issue 4, (2025) Article 15

International Journal
of
Energy and Environmental Engineering (IJEEE)

https://doi.org/10.57647/ijeee.2025.1603.15

Predictive Thermal Analysis of 500kV GIS Circuit Breakers via Coupled Multi-Field Simulation

Runkun Guo*

ShanXi Institute of Mechanical & Electrical Engineering, Chang Zhi 046011, China

***Corresponding author:** wooride@126.com & RunkuGuo648@outlook.com

Original Research

Received:
16 August 2025

Accepted:
20 November 2025

Published in Issue:
31 December 2025

Abstract

The temperature of the contacts is a crucial signal for successfully identifying thermal failures in GIS (Gas Insulated Switchgear) disconnects switches, which may cause dangerous electrical mishaps. This highlights the critical need of doing temperature field computations for GIS. In any electrical system, gas insulated switchgear (GIS) plays an essential role. The insulating gas's efficacy and the device's lifespan would be diminished if the conductor on the GIS busbar were to overheat. Subsequently, we optimize the busbar's output by adjusting its center distance, conductor thickness, and rotation angle. Gas insulated switchgear and gas insulated transmission lines are essential components of any reliable electrical system. For long-distance, high-power transmission, GILs are progressively displacing traditional overhead lines because to their lower overall cost and improved efficiency in space usage and power transfer. Studying GILs' power loss with temperature profiles is important for their dependable functioning and their design optimization ease. Variations in conductor thickness accounted for over 70% of the variation in maximum temperature as well as power loss, according to the research. Combining the aforementioned methods (A1, B5, C5) allows for a decrease in GIS thermal load and energy usage. Also, following structural adjustment, the study demonstrates that SF6 gas maintains its exceptional insulating ability. This is proven by calculating the gas breakdown margin. Finally, this work adds to our knowledge of how threephase GIS busbars conduct heat, which is useful for optimizing and designing these systems. The skin effect of current is a major contributor to the temperature of gas insulated bus bars, which are the result of linked multiphysics fields including fluid, thermal, and eddy current. This study builds a 3D model of a GIS bus bar and uses additional fine grids to account for the skin impact of current in order to get an accurate loss value. The three-phase GIS bus bar's temperature field distribution is predicted using the finite element approach in conjunction with fluid analysis. The study shows that multi-physics field coupling simulations are useful for enhancing the performance and reliability of power system components, particularly GILs, by looking at the temperature field of 500kV GIS circuit breakers. Doing so improves the efficiency and dependability of the power system's components. The primary finding of this study is that three-phase GIS busbars should be designed with optimal heat transfer and other factors in mind. A 500 kV GIS disconnect switch is modeled using a multi-

physics simulation in this article. To begin, the distribution of losses is determined by electromagnetic modeling calculations. The distributions of both the temperature and the flow field are then obtained by coupling the computed losses to the fluid field's temperature as heat sources. In anomalous contact situations, this is used as a basis for additional temperature field investigation for varied contact resistance values. According to the findings, the GIS disconnect switch's top contacts are where the majority of the temperature spikes occur. When there is insufficient contact, the maximum temperature is 45. 23 percent greater than when everything is running well. For precise analysis of the temperature field of a 500kV GIS circuit breaker, multi-physics field coupling simulation is essential.

Keywords: Gas insulated switchgears (GIS); Multi-physics field coupling simulation; Temperature field analysis; Power loss density; Three phase GIS Busbars

Cite this article: Gue, R. Predictive Thermal Analysis of 500kV GIS Circuit Breakers via Coupled Multi-Field Simulation. Int. J. Energy Environ. Eng. 2025; 16(4): Article 15. https://doi.org/10.57647/ijeee.2025.1604.15

1. Introduction

Gas Insulated Switchgear (GIS) safety is related to the IEC risk assessment standard. An integral part of the engineering discipline concerned with the transformation and transmission of electricity is gas-insulated switchgear [1], [2]. According to studies done in 2020, a GIS's functional dependability might be enhanced by reducing the busbar's operating temperature and detecting its temperature more precisely [3]. Reduced power losses and total energy usage may be achieved in GIS systems by maintaining a lower busbar temperature [4].

To forecast the increase in busbar temperature, a finite element approach based on magnetic-thermal interaction was suggested [5], [6]. This technique, which relies on the loss discovered in the magnetic field analysis to create heat in the busbar, has been shown successful in experiments [7].

Next, a multi-physics coupled GIS busbar system was developed using the finite elements approach [8]. The GIS busbar's thermal characteristics were studied using an electromagnetic-flow-thermal coupling model [9]. The researchers kept an eye on the busbar's temperature while they adjusted the conductor along with enclosure diameters. To improve heat transfer inside the GIS, it was proposed to alter the busbar conductor design by inserting holes into the conductor [10]. Because of this, the conductor's maximum temperature dropped by 4 K compared to before.

Using the SF6 gas breakdown criteria as a consideration, existing authors presented a novel approach to busbar design. The idea behind this method is to maintain a constant, hospitable temperature differential between the operating environment and the busbar conductors [11].

A finite element simulation of a common-box GIS busbar with three phases and 500Kv has been built to accomplish the goals of this study. At this point, we take into account the outcomes caused by heat radiation. For purposes of safety, it is critical to know whether the busbar will fail [12], [13].

Given the multi-physical domain connection involved in optimum GIS busbar design with GIS heat transfer calculations, this work might revolutionize the sector [14], [15].

By using this tack, we may piece together the complex web of physical processes that affects the circuit breaker's internal temperature distribution, including electrical, thermal, as well as mechanical influences. A description of the rationale and implementation of this method follows [16], [17]:

1.1. Importance of multi-physics field coupling

- **Complex Interactions:** Multiple physical mechanisms are involved in GIS circuit breakers. Among them are [18], [19]:
- **Electrical fields:** Heat and electromagnetic effects are produced by high-voltage and high-current flows.
- **Thermal fields:** The temperature of the materials around electrical components is affected by the heat they produce.
- **Mechanical fields:** The stress distribution may be impacted by expansion and contraction caused by variations in temperature, which might lead to problems.
- **Accurate Temperature Distribution:** Timely and precise study of temperature fields is crucial for [20]:
  - **Reliability:** Keeping the circuit breaker's operating temperature within acceptable ranges.
  - **Component Design:** Making parts that can endure the expected temperature changes.
  - **Safety:** Keeping the power system safe from overheating and breakdowns.

1.2. Process of multi-physics modeling

- **Coupling Different Physics**
  All sorts of physical fields may have their interactions modelled by the simulation program. As an example:
- Heat production as a result of electrical losses might be predicted by electrical field models.
- By factoring in material characteristics, heat transfer processes, and boundary conditions, thermal simulations would eventually represent the distribution of this heat within the circuit breaker.
- The stresses and strains caused by thermal expansion might impact the breaker's structural integrity; mechanical models can help examine these factors.

1.3. Numerical methods of multi-physics modeling

- **Coupling different physics:** Numerical approaches, such the FEM, are used in these simulations to resolve intricate equations that characterize the behavior of every physical field.
  The Advantages of Multi-Physical Modeling:
- **Detailed temperature profiles:** Highlights possible hotspots by providing a comprehensive map of the circuit breaker's temperature distribution
- **Improved design:** Allows engineers to improve circuit breaker designs by taking mechanical, thermal, and electrical aspects into account simultaneously
- **Reduced testing costs:** May aid in minimizing the need for rigorous physical testing by reliably forecasting the circuit breaker's behavior under different operating circumstances.

For example, in a GIS circuit breaker, a thermal simulation may simulate the heat produced by a contactor and then anticipate the breaker's internal temperature profile by analyzing the convection and conduction of this heat via the insulating gas and other components. The mechanical analysis would examine the effects of temperature fluctuations on the contactor along with other components, including their expansion and contraction, stress, and the operation of the breaker. Essentially, a potent technique for understanding the intricate behavior of 500kV GIS circuit breakers along with guaranteeing their dependable and secure functioning is multi-physics field coupling modeling.

1.4. Problem statement

The dependability and security of GIS are crucial in power transformation and transmission designs. The temperature outside has a major effect on the GIS busbar's performance and dependability. Careful measurement and reduction of the busbar's temperature increase is vital for improving GIS security and reducing wasteful energy use caused by power losses.

2. Related work

Variations in conductor thickness accounted for almost 70% of the highest temperature while power loss variations, according to researchers in [21]. Combining the aforementioned methods (A1, B5, C5) allows for a decrease in GIS thermal load and energy usage. Also, following structural adjustment, the study demonstrates that SF6 gas maintains its exceptional insulating ability. That is proven by calculating the gas breakdown margin. Finally, that work adds to their knowledge of how three-phase GIS busbars conduct heat, which is useful for engineering and optimization purposes. The study shows that multi-physics field coupling simulations are useful for enhancing the performance and reliability of power system components, particularly GILs, by looking at the temperature field of 500kV GIS circuit breakers. Doing so improves the efficiency and dependability of the power system's components. The primary conclusions drawn from that study include the optimal heat transfer as well as other aspects of three-phase GIS busbar design.

The experimentalists in [22] built a model for the circuit breaker opening process that incorporates multiple physics fields, ran simulations to determine the opening process, analyzed the flow characteristics within the interrupting chamber during various opening processes, and obtained distribution and change trends of parameters like electric field, temperature, density, pressure, while airflow speed. In order to set up fault diagnostics using the digital twin of the circuit breaker, they choose the defining characteristics and provide the necessary data. By simulating overvoltage & surge current scenarios that could occur throughout the switching process of a shunt capacitor bank, the researchers in [23] were able to determine why reactive power compensating SF6 circuit breakers had such a high resistance in real-world switching scenarios. A multi-physics field simulation was then run on the arc chamber's electromagnetic field, temperature field, as well as fluid field coupling using overvoltage and surge current data. According to the findings, the surge current produced when connecting the shunt capacitor bank may exceed 16. 8 times the rated current, and the reignition overvoltage during disconnection can reach 6 times the system's rated voltage. These factors considerably affect the circuit breaker's ability to operate steadily. A temperature increase of up to around 1000K is possible as a result of the surge current that is created during the connecting procedure.

The contact may become as hot as 7875 K thanks to the reignited arc, which can burn it. The electrical contact efficiency of the contacts will be affected by all of these scenarios, leading to breaker circuit resistance exceeding the norm. The multi-physics field simulation for ±550kV DC GIS RCVD was developed by the authors of [24] using the research technique of "field distribution analysis stray variable analysis field-circuit coupling accuracy of measurement analysis. " The RCVD's circuit model for calculating measurement accuracy is developed, and the effect of the distribution of electrostatic as well as thermal fields on measurement accuracy is studied. That effort may point researchers in the right path as they attempt to advance high-precision RCVD. Equipped with conductive or insulated conductive components, the authors of [25] developed a mathematical model for electrothermal coupling. That model is numerically solved using ANSYS - multi physics.

The impact of heat sources like contact resistance while bridge resistance on the temperature rise is examined. The impact of the convection heat transfer coefficients on the temperature rise is addressed.

The impact of the thermal insulation layer's area, thickness, and thermal conductivity on the temperatures rise of the cavity is emphasized. The accuracy of the 3 kA through-flow rise in temperature calculation while the measured data were determined to be within the project's allowable range, demonstrating that the mathematical model while theoretical analysis were correct, after which a high-speed breaker prototype was developed.

A high-speed breaker solution was developed, successfully resolving the technical issues with the target power system. It had an overall resistance of 13. 3 μΩ, a temperature increase of 30k for the terminal copper bar, with an increase in temperature of 40k for the cavity.

3. Three-phase gas-insulated switchgear (GIS) busbar system

Power distribution in GIS switchgear relies on a Three-Phase Gas Insulated Busbar (GIS) technology. To make sure it works reliably and safely, it has a metal housing that is filled with insulating gas, usually sulfur hexafluoride (SF6).

The system's three phase conductors are often placed in an inverted triangle arrangement for best performance.

If there is a problem or overload in a three-phase GIS bus bar structure, the current will be cut off by a circuit breaker.

Because GIS systems often use high voltages and currents, these circuit breakers are specifically designed to handle them. Gas insulation provides better insulation and arc suppression than air insulation; hence these switchgears are usually housed in a sealed, gas-insulated enclosure, which is depicted in Figure 1.

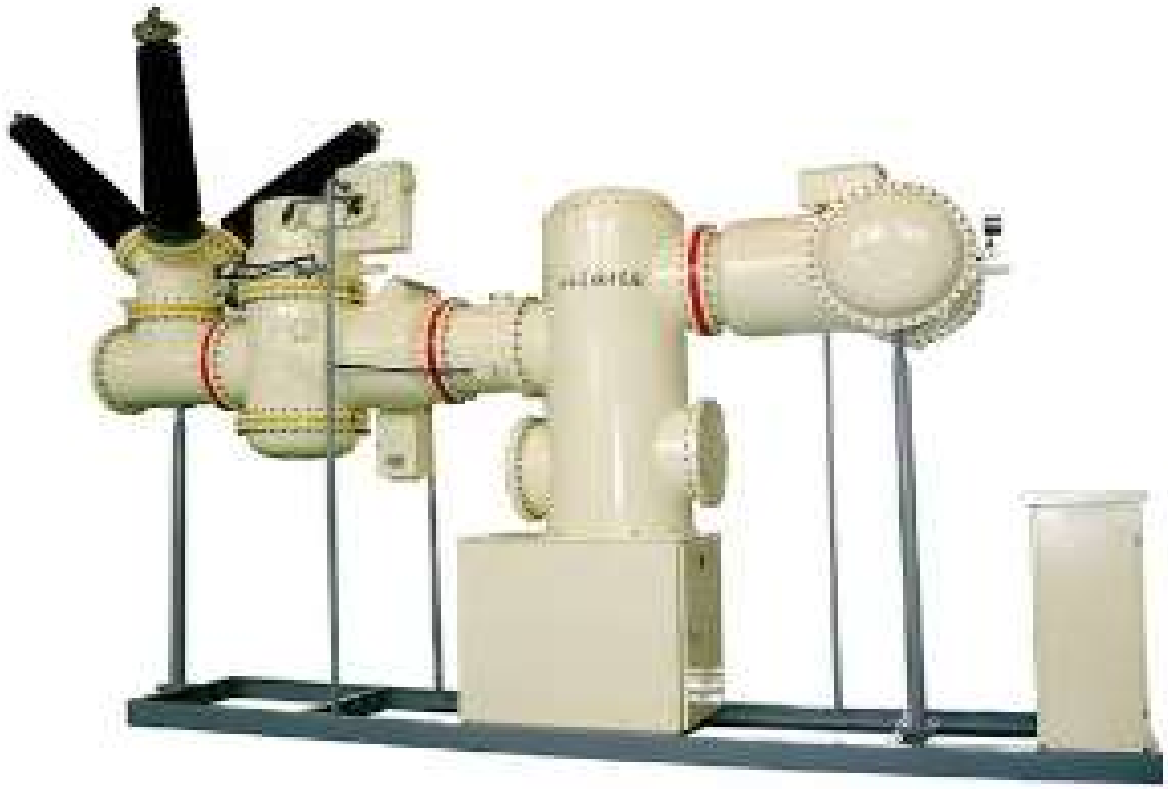

Figure 1. Outdoor Sf6 Gas-Insulated Switchgear (GIS)

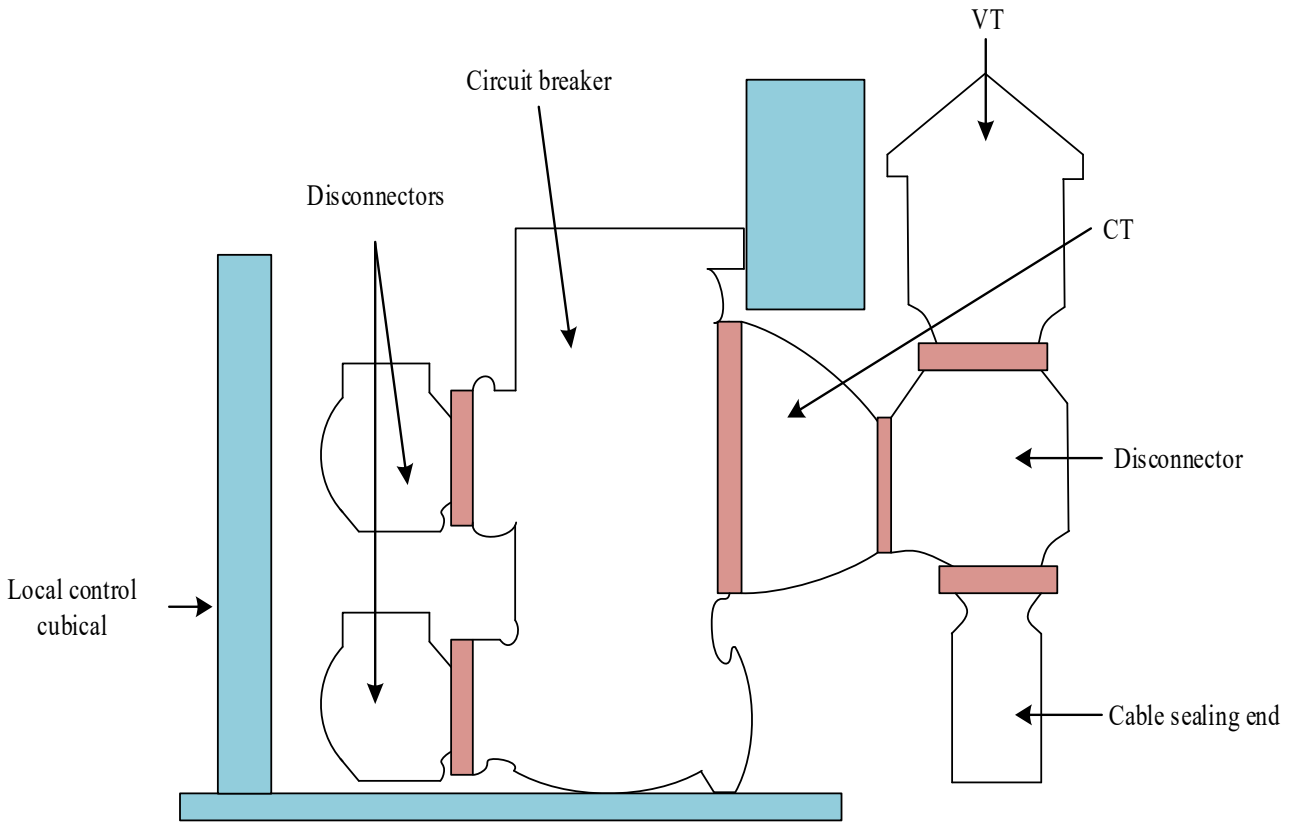

Figure 2. GIS Circuit Breaker Model

Figure 2 shows the GIS circuit breaker model for temperature analysis in three bus bar system model.

3.1. Key features and components

- **Enclosure:** Encased in a metal housing, the insulating gas shields the living components from harm.
- **Three-Phase Conductors:** These wires, usually laid out in an inverted triangular pattern, carry the electricity.
- **Insulating Gas (SF6):** When compared to air, the gas's arc-quenching and insulating properties make it the more reliable option.
- **Spacers:** These fasteners secure the three-phase wires within the housing.
- **Branch Bus:** Additional equipment may be connected to a branch bus that extends upwards from the main conductor.

GIS busbar systems are widely used in:

- **Power Substations:** With the purpose of distributing power in distribution and transmission networks.
- **Industrial Plants:** In fields where room is at a premium and dependability is paramount.
- **Utilities:** In places that generate and distribute electricity.

Circuit breaker types in GIS

- **SF6 Gas-Insulated Circuit Breakers:** Popular because of how well they work and how reliable they are.
- **Vacuum Circuit Breakers:**A vacuum-operated GIS circuit breaker is a further kind.

3.2. GIS circuit modeling

The conductors of SF6 gas and busbars are affected by temperature. The specific heat capacity as well as thermal conductivity of SF6 gas are given by Eqs. (1) and (2), respectively.

This has been verified by a number of investigations (18). The Tenv of room temperature air is 290 K, but the Sutherland constant (S) of SF6 gas is 110. 55 K.

$$c_{p,sf6}(T) = -2 \times 10^{-3} \times T^2 + 2.4 \times T + 123.4 \quad (1)$$

$$\gamma_{sf6} = 0.01206 \times (T/T_{env})^{1.5} \times \left((T_{env} + S)/(T + S)\right) \quad (2)$$

The electrical conductivity of busbar conductors is represented by the numerical value 2 (T) according to Eq. (3).

$$\sigma(T) = 1/p_0\left(1 + \alpha(T - T_{ref})\right) \quad (3)$$

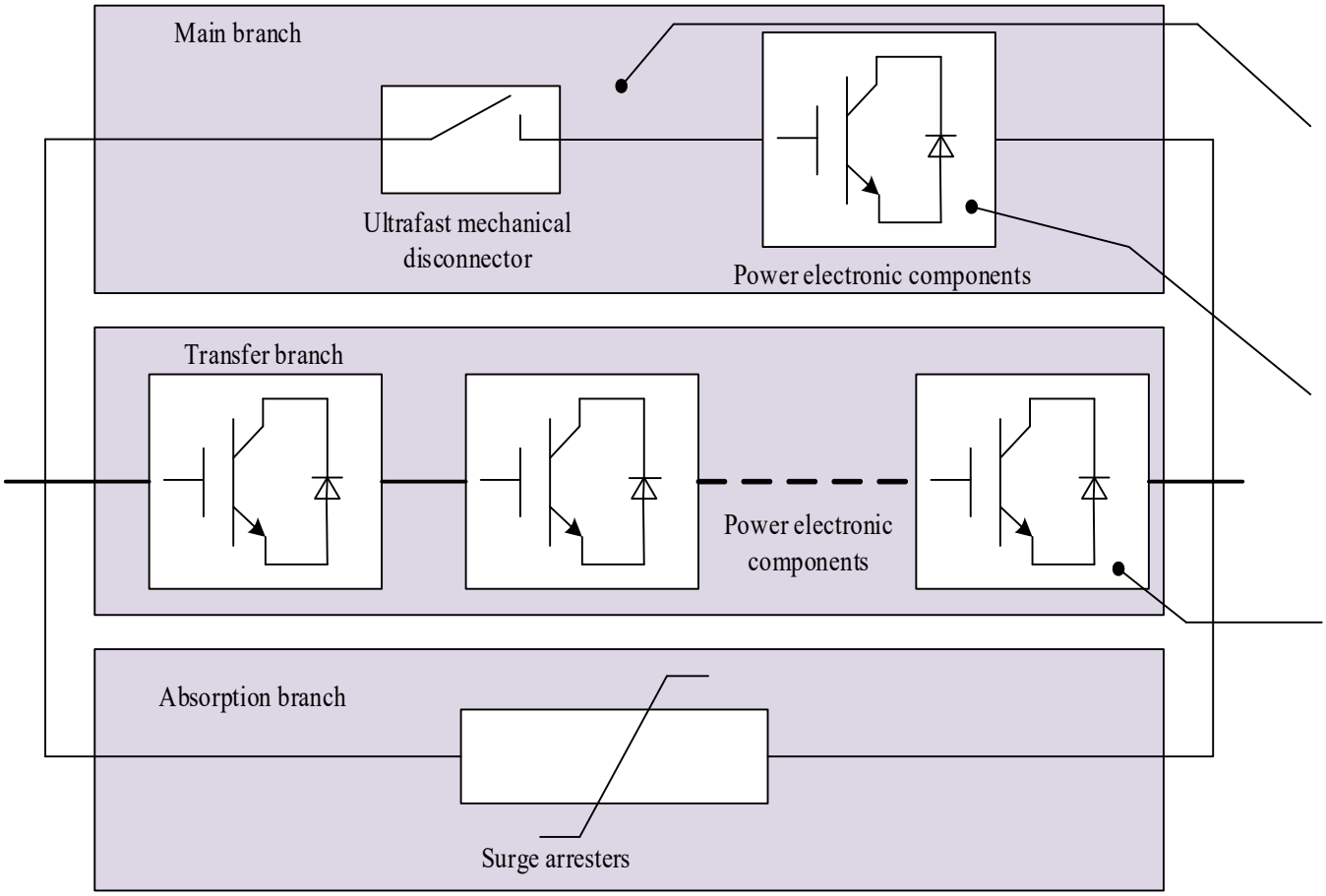

Figure 3. Circuit Breaker in Model

Figure 3 shows the typical circuit breaker model by using power electronic components

3.3. Approaches to control equation calculation

In the GIS model, the solid domain consists of the enclosure and conductors, while the fluid domain is the SF6 gas. The solid-domain electromagnetic-heat coupling is denoted using Eqs. (4) through (6). Eq. (5), the magnetic loss equation, connects Eqs. 4 and 5.

$$\nabla \cdot (\gamma(T)\nabla T) + Q_e = 0$$

$$Q_e = Q_{rh} + Q_{ml} = \frac{1}{2}\mathrm{Re}(\vec{J} \cdot \vec{E}) + \frac{1}{2}\mathrm{Re}(j\omega\vec{B} \cdot \vec{H}) \quad (4)$$

$$-\omega^2\gamma\vec{A} + j\omega\sigma(T)\vec{A} + \nabla \times \left(u^{-1}\nabla \times \vec{A}\right) = 0 \quad (5)$$

Eqs (7-9) depict the constitutive laws of the electromagnetic field.

$$\nabla \times \vec{A} = \vec{B} \quad (6)$$

$$\vec{E} = -j\omega\vec{A} \quad (7)$$

$$\vec{B} = u\vec{H} \quad (8)$$

$$\vec{J} = \sigma(T)\vec{E} \quad (9)$$

The thermal characteristics of SF6 gas, as calculated using COMSOL finite element modeling software, link Eqs. 11, 12, and 13.

Eqs. (11)–(13) outline the coupled heat-flow dynamics of the fluid domain.

$$\nabla_{\vec{V}} = 0 \quad (10)$$

$$P(T)(\vec{v} \cdot \nabla T) = \nabla \cdot \left[\left(\frac{\gamma(T)}{c_p} + \frac{u_t}{\sigma_T}\right) \cdot (\nabla T)\right] \quad (11)$$

$$p(T)(\vec{v}.\nabla_{\vec{v}}) = -\nabla p + \nabla.\left[(u(T) + u_t)\left(\nabla_{\vec{v}} + \left(\nabla_{\vec{V}}\right)^T\right)\right. \quad (12)$$

Here, T is the thermal conductivity, which is a measure of the heat transmission from the GIS enclosure to the busbar conductors in watts per meter-Kelvin. A radiative emissivity of 0. 85 is seen in the k and c bands. At a temperature of 290 °K, the convection outside a horizontal cylindrical wall is the heat transfer mechanism along the outside of the GIS enclosure. The present inquiry's governing equations are solved using the MUMPS solvers in COMSOL Multiphysics 5. 2.

Figure 4. GIS Model Scene

Table 1. The 500 kV GIS disconnector's parameters

Parameter	Value (mm)	Parameter	Value
Fracture distance	190	Rated pressure/MPa	0. 7
Contact radius	80	Rated voltage/kV	500
Shield radius	190	Rated current/kA	5
Inside diameter of shell	1200	Open speed m s $^{-1}$	4
Outside diameter of shell	1140		

3.4. Mathematical model and computational methods

Formula (2) makes it clear that determining the minimal density point when the circuit breaker is in operation is the most important step in determining the critical breakdown field strength. The density distribution for SF6 gas in GIS remains essentially constant under typical operating conditions because to the equilibrium between gas flow and heat transfer. After the SF6 gas begins to flow when the circuit breaker is turned on, the heat transfer-gas flow balance is disrupted, and the density distribution varies with the changes in the moving contact until the process is complete. To construct a mathematical model depicting the fluid for flow that is compressible, the N-S equations are optimal for gas flow, which is given in Figure 4.

The previous model treats SF_6 as if it were a perfect gas, ignoring the compression factor that indicates the density deviation. Eq. (16) represents the gas density under a certain pressure and temperature; it is used in Eq. (14) in section II B when taking compression factor into account.

$$\rho(T) = \frac{PM}{ZRT} \tag{13}$$

Eq. (16) depicts the density of ideal gas when Z=1, whereby Z is the compression factor.

One way to get the gas compression factor at a given temperature and pressure is to iteratively solve the Soave-Redlich-Kwong (SRK) equation. Soave built the SRK equation on top of the Redlich-Kwong equation; it incorporates the gas eccentric component and offers accurate calculations for both pure and mixed gases with several components.

To express the iterative SRK equation in terms of gas conditions (temperature and pressure), one uses

$$\begin{cases} Z = \dfrac{1}{1 - bP/ZT} + \dfrac{a(T)}{bRT}\dfrac{1}{1 - ZT/bP} \\ b = 0.08664\dfrac{T_c}{P_c} \\ a(T) = 0.42748\dfrac{R^2T_c}{P_c}[1 + 0.80278(1 - T_r^{0.5})] \end{cases} \tag{14}$$

the reduced temperature (T_r), the critical pressure (P_c), and the critical temperature (T_c) are defined, accordingly.

Here is the iteration process:

- With a starting compression factor of 1, we can begin.
- The multi-physical field coupling simulation is used to determine the average temperature of the SF_6 gas.
- Eq. (17) is used to calculate and update the compression factor.
- After running the model several times, we can obtain the convergence value of the average temperature of the gas and its corresponded compression factor.

The conditions used for the simulation in this work include a gas pressure of 0. 6 MPa, a current of 3000A, and a phase voltage of 289 kV.

3.5. Temperature analysis

An effect known as the skin effect occurs when an alternating current passes through a conductor's cross section and the current density is distributed unevenly over that cross section. The skin effect calculation is shown using a single conductor model. Its copper construction allows for a current of 10 kiloamperes (kA) at a frequency of 50 hertz, and its dimensions are 0. 4 meters in radius with 2 meters in axial length. The air domain border is sufficiently far in this model to guarantee logic. This conductor has a deep length of skin impact of 9. 35 mm, this is defined by the following formula involving frequency, conductivity, and magneto conductivity:

$$\delta = \sqrt{\frac{2\rho}{\omega\mu}} \tag{15}$$

Eq. 15 depicts the distribution of current densities; it reveals that the current is concentrated on the conductor's surface and reaches its maximum near its extremes. The Reynolds coefficient is a defining parameter that classifies fluid flows as either laminar or turbulent. Flow is considered laminar when the Reynolds coefficient is below 2300 and turbulent when it is more than or equal to 2300. With a viscosity coefficient of SF_6 on the order of 10^(-5), and a typical size of the gas flow channel among contacts of about 10^(-1) " " m for 550 kV GIS, we may roughly calculate the value of the Reynolds coefficient in the flow region of the disconnector chamber. The end effect is that the Reynolds coefficient is far higher than 2300, at around 10^4. So, SF_6 gas in the disconnector chamber could be considered to be flowing turbulently and transferring heat. Here we establish the governing equations for natural convection and transfer:

(1) Formula for the conservation of mass

$$\nabla \cdot (\rho u) = 0 \tag{16}$$

(2) Equation for the conservation of momentum

$$\rho(u \cdot \nabla)u = \nabla \cdot \left[-pI + \mu_{gas}(\nabla u + (\nabla u)^T) - \frac{2}{3}\mu_{gas}(\nabla u)I\right] + g\Delta\rho \tag{17}$$

(3) Conservation of energy formula

$$\rho c_p u \nabla T = \nabla \cdot (k\nabla T) + Q \tag{18}$$

Where, ρ is density; c_p includes the variables k (specific heat capacity), u (velocity vector), p (pressure), and T (temperature), C; μ_{gas} $\Delta\rho$ represents the density differential of gas, I stand for unit matrix, g stands for acceleration of gravity, and is the gas's viscosity. The power source word is Q.

Aside from the obvious differences in current density at the periphery, the two grid split schemes also exhibit noticeable differences in the maximum current density. In Figure 3, path 2 shows that when the conductor is separated into one layer, the electrical current density briefly increases as it moves from the edges to the center, then immediately decreases; this entire process resembles a parabolic shape. However, when the conductor is divided into two layers, the current density completely goes into a monotonically decreasing state. If the electromagnetic energy error falls below 0. 007%, the analysis is essentially stopped in this study's convergence procedure.

(2) Boundary condition

Both the velocity field and the temperature field serve as boundaries.

(1) Temperature field boundary

a) Outside surface of contact

$$-k_1\frac{\partial T}{\partial n} = \alpha_{in}(T_{cont} - T_{encl}) + \varepsilon_{in}\sigma_b(T_{cont}^4 - T_{encl}^4) \tag{19}$$

b) Surface outside the enclosure

$$-k_2\frac{\partial T}{\partial n} = \alpha_{out}(T_{encl} - T_{surr}) + \varepsilon_{out}\sigma_b(T_{end}^4 - T_{surr}^4) \tag{20}$$

Where, k_1 and k_2 for the GIS shell and the contact heat conductivity coefficient, respectively.

α_{in} and α_{out} refers to the contact's convective heat dissipation coefficient and the GIS shell's coefficient, respectively. T_{cont}, T_{end} and T_{surr} is the temperature of contact, whereas the temperature of the enclosure and the outside environment are, respectively. ε_{in} and ε_{out} as well as the radiation coefficient of enclosure, which are comparable, respectively.

The Stefan-Boltzmann constant is denoted by σ_b, $\sigma_b = 5.67 \times 10^{-8}\ W/(m^2.K^4)$

(2) Velocity boundary condition

For SF_6 On the surface of SF_6, gas has, because the flow boundary is defined by the no-slip velocity boundary conditions.

$$u_{surf} = v_{surf} = w_{surf} = 0 \quad (21)$$

Where, $u_{surf}, v_{surf}, w_{surf}$ is the speed in the x, y, and z directions of the gas fluid SF_6 on the surface of the interior of the GIS shell.

(3) Initial conditions

A system's starting point consists of three variables: velocity, pressure, and temperature.

$$\begin{cases} T = 20°C \\ u = v = w = 0 \\ p = 0.5MPa \end{cases} \quad (22)$$

In where u, v, and w are the velocities of the SF_6 gas fluid in the x, y, and Z dimensions, respectively.

3.6. Temperature rise governing equation

Eq. (10), which presents the energy conservation equation, shows how the temperature field and the flow field are coupled. The following equation is used to calculate the temperature increase of SF_6 gas in the disconnector chamber,

$$\frac{\partial}{\partial x}\left(k\frac{\partial T}{\partial x}\right) + \frac{\partial}{\partial y}\left(k\frac{\partial T}{\partial y}\right) + \frac{\partial}{\partial z}\left(k\frac{\partial T}{\partial z}\right) + q_v = \rho c_P \frac{\partial T}{\partial t} \quad (23)$$

Where, q_v calculates the amount of heat produced by a given volume in relation to time, $/(m^3 \cdot s)$. The resistance effect causes the conductor to get heated as the current flows through it. The ohmic heat effect describes this kind of thermal phenomenon. That an alternating electric field may produce an alternating magnetic field is familiar to everyone. The process of electromagnetic induction states that an alternating magnetic field may produce an induced current, which then runs through a conductor and causes it to heat up, leading to a loss of power. A phenomenon known as loss of eddy current describes this sort of power loss.

To summarize, the disconnector chamber experiences two types of heat: ohmic heat as well as eddy current loss.

3.7. Eddy current loss

You may figure out the eddy current loss by using this formula:

$$\frac{1}{\mu}\nabla^2\vec{A} - \sigma\frac{\partial\vec{A}}{\partial t} = -J_e \quad (24)$$

A, magnetic vector potential, μ, electrical conductivity, and J_e, volume density of current induced are all variables in this context.

Thermal radiation, convection heat dissipation, and heat conduction are the primary modes of heat transmission for insulating gas encased conductors with current following.

Natural convection is quite important within GIS bus hars, and the impact of heat radiation is negligible. Two main players on the enclosure's surface are convection and heat radiation. Here is the equation for thermal balance:

$$P_c + P_e = Q_{ec} + Q_{er}$$
$$P_c = Q_{cec} + Q_{cer} \quad (25)$$

Where P_c and P_e are the enclosure's power loss and the bus bars' power loss, respectively, Q_α and Q_σ dissipate heat by radiation and conduction between the container and the ambient air.

Q_{ec} and Q_{cer} are the heat transfer coefficients for convection and radiation, respectively, between the enclosure and the conductor.

3.8. Dynamic circuit breaker analysis of SF_6 gas discharge

Information fitting technology is used to examine the impact of switching operating circumstances on the dynamic breakdown features of the SF6 gas discharge, with the goal of gaining a comprehensive understanding of this feature.

In most cases, two guidelines for data fitting are taken into account.

(1) F-Test Analysis: The relevance of the fitting expression is commonly checked using P for the F test technique. The fitting impact is poor and the result is not statistically significant if p>0. 05.

(2) R^2 criterion: R^2 is the goodness of fit, a measure for evaluating the degree of fit. The closer the value of R^2 is to 1, the better the fit. In most cases, a goodness value higher than 0. 9 is necessary. The following equation may be used to produce R^2,

$$R^2 = 1 - \frac{SSE}{SST} \quad (26)$$

Thus, SSE is the total sum of squares, whereas SST is the sum of residuals.

3.9. Finite-element method

Contact temperatures in three-phase gas-insulated busbars (GIBs) may be predicted using the Finite Element Method (FEM), a computational approach. When used in conjunction with CFD, this technique can model the GIB's heat distribution, fluid flow, and eddy currents in three dimensions. Important for GIB status tracking and failure prevention due to overheating, FEM can precisely anticipate temperature increase at the contacts through modeling the contact resistance while taking into account the temperature-dependent characteristics of SF6 gas and air.

Modeling the GIB:

- **3D Geometry:** Using FEM, a three-dimensional model of the GIB is created, which includes the gas, enclosure, and conductors.
- **Contact Resistance**: larger distance between the conductor with the contact, indicating that the passage of current is constrained.
- **Temperature Dependence:** Thermal analysis takes into account the fact that the thermal characteristics of SF6 gas and air are thought to be temperature-dependent.

4. Experimental model

Both the mechanical stress and the magnetic field force are modelled and evaluated using the traditional ANSYS finite elements analysis program. A 3D Multi-Physics coupling framework (temperature-flow-electromagnetic field) is developed to determine the dynamic density shifting of SF6 gas discharge while the disconnector switching, which is the main emphasis of this research. The breakdown field strength is then mathematically expressed using the linear regression fitting approach. In addition, the dynamic breakdown properties of SF6 gas throughout disconnector switching are effectively determined, and the discussion expands to include the circuit breaker operating conditions that impact these features.

4.1. Model validation

A mesh that is too fine makes computation impossible with the multi-physics direct coupling method, which demands an extremely large amount of memory resources. The present study compared four distinct grid layouts for their efficacy. The sum of the four sets' grid counts is 13132, with 6000, 7754, 10064, as well as 13132 grids in each. If you want your simulation to be accurate, you need to check the calculating model and process. The typical box GIS heat transfer model, which is three-phase, is used in the verification process. Three thousand amperes are the rated current, while sixty hertz is the rate of the alternating current. Based on the results, it seems safe to use the mathematical model and approach used in this research.

4.2. Results and discussion

Experimental data of temperature increase from a 500 kV three-phase GIB prototype are compared with the predictions of the FEM model to confirm its correctness. By using the established approach to GIB condition monitoring, anomalous contact conditions may be detected early and failures can be prevented. The distribution of temperatures inside the GIB is predicted by combining the effects of eddy currents, fluid movement, and thermal characteristics. To avoid overheating and guarantee dependable operation, engineers may design GIBs with suitable cooling systems as well as materials by estimating the temperature increase at the contacts. By combining FEM with CFD, a potent tool is created for the prediction and understanding of the thermal behavior of three-phase GIBs. This, in turn, leads to power transmission systems that are more dependable and efficient. Using numerical modeling with the Taguchi approach, we find the best design specifications for a three-phase GIS busbar that uses 252 kV and a 3150 A load. Our goal in doing this is to determine the optimal setup for a 252 kV three-phase GIS busbar. In this case, (d0) is the distance among the center of the conductor and the center of the GIS, and () is the thickness of the conductor; all three are spinning at the identical rate. There are five categories that each optimized parameter fits within, as shown in Table 1.

Table 1. Optimized parameters

Optimized Parameter	Symbols	Level				
$\emptyset$	A	0	32	56	49	82
d_0	B	62	88	125	141	167
φ	C	8	13	15	23	31

Isolating the effects of each variable causes the analysis's overall cost to skyrocket. The number of simulations should be 25. Find the signal-to-noise ratio (SNR) by using the highest temperature (Tmax). The value of the performance statistic (PS_{ij}) is the SNR averaged across all instances when the optimized parameter (, d0,) was used. Adjusting the settings resulted in optimum PS_{ij} values, which are detailed in Table 2. The negative value in the SNR calculation procedure indicates that the highest temperature or power loss is reduced when PS_{ij} is bigger.

$$R_1 = max(PS_{ij} \mid j = 1,2,3,4,5)\ CR_i = R_i/\sum_i^3 R_i \quad (27)$$

Table 2. Performance statistics

Target	Optimized Parameter	Psi. j						
		Level 1	Level 2	Level 3	Level 4	Level 5		
T_{max}	A	-243.8	-247.7	-262.9	-241.6	-264.8	0.14	8.9%
	B	-262.5	-263.3	-274.5	-244.3	-288.1	0.24	23.1%
	C	-267.6	-264.8	-243.8	-266.8	-264.2	1.43	67%
Q_h	A	-289.8	-285.1	-265.2	-276.1	-261.3	0.67	6.9%
	B	-267.3	-282.3	-284.6	-283.5	-294.4	1.67	23%
	C	-264.4	-269.6	-261.9	-258.8	-264.2	6.45	69.7%

Tmax and Qh are also determined by the conductor thickness, as shown in Table 2. By factoring in conductor thickness, we can build a high-quality three-phase GIS busbar. If we determine the ideal central distance, d0, we can cut power loss by 20. 7% and peak temperature by 21. 5%. Because of its great degree of flexibility, it may be adjusted to meet your unique needs. Rotating the conductor has a negligible effect on temperature and loss (less than 10% change). Data from the best performance level of parameter A indicates that its maximum temperature (Tmax) is at its lowest if the rotation angle is zero. The optimal both B and C values are found at Level 5. (A1, B5, C5) is the most effective in reducing the maximum temperature of the GIS busbar that does not exceed the limits of the investigation. For the unoptimized design (=0, d0=140 mm, =15 mm), the GIS power loss density (Qh), the SF6 gas average velocity (Uave), with the busbar maximum temperature (Tmax) are shown in Table 3. Flow fields are vertically symmetrical due to gravity and confinement. At the wall's edges, the flow field reaches its maximum velocity. Even though the heat is distributed evenly over the busbar, the maximum temperature is seen in conductor A. The breakdown margin is lowest in the auxiliary sections of the three busbar conductors when an electric field is high and SF6 gas is flowing. Because of electric fields, this happens.

Table 3. Comparison of optimum conditions

Conditions	U_{ave}	T_{max}	Q_h	E_{min}
$\Theta = 0, do = 130$ mm	0. 056	433. 5	867. 2	8. 12
$\Theta = 0, do = 150$ mm	0. 045	421. 1	499. 3	4. 23

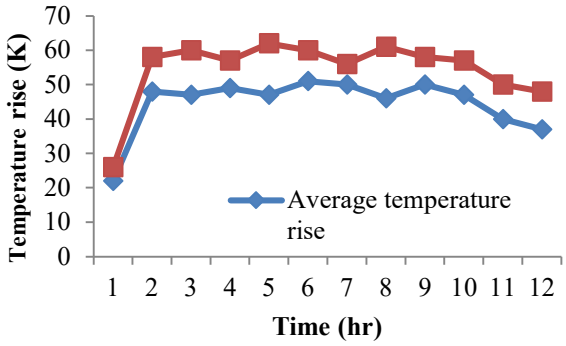

Figure 5. Temperature Rise Analysis

By comparing the outcomes before and after optimizing, you can see that the former yields better results. Nothing has changed with respect to the rules of distribution for the temperature field, breakdown margin, and flow field (1). Findings reveal a 50K average winding temperature jump and a 63K hot spot temperature spike, according to the research.

An acceptable structural design is shown by the fact that the temperature rise within every enclosure climbs gradually from bottom to top, with the outermost and innermost envelopes having noticeably lower temperature rises and the remaining envelopes having uniformly distributed temperatures. As shown by the simulation results:

- Even if the tension on a single arm encapsulation diminishes as it moves outward, some of those arms will rebound, and the deformation of the encapsulation will be greater in the center than on the inside.
- The highest stress level is 70 MPa, the largest deformation is 0. 60 mm, while the safety factor is 1. 5

5. Conclusion

A Three-Phase GIS Busbar was designed utilizing data collected before and after Taguchi optimization. In order to find the best outcome, this is done. The most significant discoveries are listed below, in chronological order: Several variables influence the highest temperature and the GIS's power loss. Nearly 70% of the effect is due to variations in conductor thickness, 20% to differences in center distance, and less than 10% to variations in rotational angle. There was no change to the SF6 gas's insulating properties; however there was a 9.56 K reduction in maximum temperature and a 158. 42 W/m² reductions in power loss density or 21. 7%. The article's physical model is simplistic; therefore the findings may not be reflective of reality. Nevertheless, the results may be used to enhance the architecture of a three-phase GIS busbar systems. This might happen regardless of whether the article's results help in designing a better three-phase GIS busbar network. If the GIS busbar framework is refined further, it could be

helpful to include contact resistance. Maximum temperature while power loss might be predicted with higher precision. In order to forecast the spatial distribution of both velocity and temperature vectors, this research sets up a three-dimensional model of GIS bus bars and couples the eddy current field with fluent-thermal. We also fine-mesh the skin impact region to ensure accurate loss of eddy current calculations. A single-phase conductor explains how to account for the skin effect. The fluid analysis then makes use of the loss as a heat source. There is a strong agreement between the temperature distribution and the distribution of the SF6 gas velocity vector for the three-phase GIS bus bar.

DECLARATION

Ethics approval and consent to participate: I confirm that all the research meets ethical guidelines and adheres to the legal requirements of the study country.

Consent for publication: I confirm that any participants (or their guardians if unable to give informed consent, or next of kin, if deceased) who may be identifiable through the manuscript (such as a case report), have been given an opportunity to review the final manuscript and have provided written consent to publish.

All authors have seen and agree with the contents of the manuscript and there is no financial interest to report. We certify that the submission is original work and is not under review at any other publication.

Funding: No funding.

Acknowledgements: All authors contributed to the study conception and design. All authors read and approved the final manuscript.

Authors Contribution
All authors contributed to the study conception and design. All authors read and approved the final manuscript. There is no human participate involved in this research. this article manuscript is created from collection of data set.

Availability of data and materials
The data used to support the findings of this study are available from the corresponding author upon request.

Conflict of interests
Here are no have no conflicts of interest to declare.

References

1. Cao, X. , Jiang, M. , Yan, Y. , Wang, Z. , Wang, B. , & Xiao, L. (2024). Analysis of a breakdown failure of 550 kV GIS circuit breaker. International Symposium on Sensors, Mechatronics, and Automation.
2. Wang, J. , Guo, H. , Yuang, L. , & Di, N. (2024). Typical Fault Analysis of SF6 Gas Insulated Metal Enclosed Circuit Breaker Compartment. 2024 International Conference on HVDC (HVDC), 477-481.
3. Zeng-jie, Y. (2010). Analysis on fault of control circuit of 500kV GIS breaker and treatment.
4. Zhang, D. , Hu, X. , Zhang, H. , Yu, H. , & Shen, Y. (2020). Ferroresonance Analysis of 500kV GIS Substation during Commissioning Process. IOP Conference Series: Earth and Environmental Science, 514.
5. Dai-ning, Z. (2012). Accident Analysis for a Unsuccessful 500kV Circuit Breaker Reclosing. High Voltage Apparatus.
6. Lei, J. , Zhong, J. , Wu, S. , Wang, Z. , Guo, Y. , & Qin, X. (2016). A 3-D Steady-State Analysis of Thermal Behavior in EHV GIS Busbar. Journal of Electrical Engineering & Technology, 11, 781-789.
7. Wang, X. , Xu, D. S. , Wang, Y. , Li, L. , Zhang, Q. J. , Lan, Q. , Lu, Y. , & Li, H. (2014). Analysis and Thoughts on a 500kV H-GIS Equipment Failure. Advanced Materials Research, 960-961, 871 - 876.
8. Wang, L. , Ma, Y. , Bao, Z. , Chen, Y. , Ren, J. , & Zhang, G. (2025). Simulation study on steady-state temperature rise distribution of helical spring contact based on electric-thermo-mechanical coupling. Journal of Physics: Conference Series, 2935.
9. Fuhai, L. , Zhan, T. , Yongqiang, D. , Yeyuan, L. , & Shi-peng, L. (2019). Analysis and Discussion on the Current Situation of SF6 Relay Temperature Compensation Mode. IOP Conference Series: Earth and Environmental Science, 310.
10. Guang-yi, Q. (2010). Introduction to In Situ Overhaul of 500kV GIS Circuit Breaker.
11. Zhang, B. , Guo, Y. , Yao, Y. , Wang, Z. , & Zhang, H. (2018). Optimization Design of Heater for GIS Circuit Breaker in Alpine Region Based on Thermal and Flow Field Coupling Simulation. DEStech Transactions on Computer Science and Engineering.
12. Wang, J. , Guo, H. , Yuang, L. , & Di, N. (2024). Typical Fault Analysis of SF6 Gas Insulated Metal Enclosed Circuit Breaker Compartment. 2024 International Conference on HVDC (HVDC), 477-481.
13. Zeng-jie, Y. (2010). Analysis on fault of control circuit of 500kV GIS breaker and treatment.
14. Cuguz, V. , Xu, G. H. , & Morf, S. (2022). A 500kV AIS Switchyard Renewal In Ontario, Canada, using 500/800kV Hybrid GIS. 2022 IEEE/PES Transmission and Distribution Conference and Exposition (T&D), 1-5.
15. Huang, L. , Fang, C. , Li, W. , Tang, X. , Zhang, N. , & Chen, J. (2020). Research on motion characteristics and stability of 500kV fast mechanical switch. Journal of Physics: Conference Series, 1633.
16. Wang, X. , Xu, D. S. , Wang, Y. , Li, L. , Zhang, Q. J. , Lan, Q. , Lu, Y. , & Li, H. (2014). Analysis and Thoughts on a 500kV H-GIS Equipment Failure. Advanced Materials Research, 960-961, 871 - 876.
17. Song, H. , Hou, G. , Wang, W. , Deng, X. , Huang, Q. , Mo, W. , Hasegawa, M. , & Li, X. (2017). Application of computational fluid dynamics to predict the temperature-rise of gas insulated switchgears. 2017 4th International Conference on Electric Power Equipment - Switching Technology (ICEPE-ST), 694-697.

18. Kobayashi, T. , Murase, H. , Nishiwaki, S. , & Kosakada, M. (2002). Time Constant of Charge Decay in 500kV Transmission Line. Ieej Transactions on Power and Energy, 122, 675-683.

19. Fuhai, L. , Zhan, T. , Yongqiang, D. , Yeyuan, L. , & Shi-peng, L. (2019). Analysis and Discussion on the Current Situation of SF6 Relay Temperature Compensation Mode. IOP Conference Series: Earth and Environmental Science, 310.

20. Bölter, F. , Israel, T. , & Kufner, T. (2023). Behavior of Electrical Contact Elements for High Current Applications during Relative axial Motion. 2023 IEEE 68th Holm Conference on Electrical Contacts (HOLM), 1-8.

21. Huang, Y. (2024). Research on the Application of Multi-Physics Field Coupling Simulation in the Analysis of Temperature Field of 500kv GIS Circuit Breaker. Journal of Electrical Systems.

22. Chen, J. , Zhang, K. , Liang, Z. , Du, Z. , & Zhang, H. (2022). Digital twin-oriented multi-physics field simulation analysis of high-voltage SF6 circuit breakers. Journal of Physics: Conference Series, 2409.

23. Jiang, Y. , Huang, K. , Zhang, K. , Cao, R. , Zhang, Q. , & Tong, Z. (2024). Multiphysics Simulation Analysis of Excessive Circuit Resistance of Reactive Power Compensation Circuit Breaker. 2024 7th International Conference on Electric Power Equipment - Switching Technology (ICEPE-ST), 754-759.

24. Zuo, Y. , Sun, H. , Ding, Y. , Xiao, J. , & Lu, Y. (2024). Multi-physical Field Model and Measurement Accuracy Error Analysis for DC GIS Resistorcapacitor Voltage Dividers. 2024 7th International Conference on Energy, Electrical and Power Engineering (CEEPE), 1068-1073.

25. Zhifang, Y. , Zhaolong, S. , & Yang, G. (2018). Modeling Analysis and Experiment of Electrothermal Coupling Characteristics of Large Current and High-Speed Breaker. 2018 2nd IEEE Conference on Energy Internet and Energy System Integration (EI2), 1-6.